Tellus (1995), 47A, 561–574
Printed in Belgium – all rights reserved

TELLUS
ISSN 0280–6495

A 30-day oscillation over the North Atlantic

Observation and simulation

By JUHANI RINNE* and SIMO JÄRVENOJA, *Finnish Meteorological Institute, PO Box 503, 00101 Helsinki, Finland*

(Manuscript received 15 September 1994; in final form 27 February 1995)

ABSTRACT

A spectral peak at a period of 30 days found in a certain EOF series is studied. A westward-moving wave local to the North Atlantic has been found. The wave is often present and is rather intense. In half of the cases, it is associated with a blocking. The wave can then be described as a retrograde blocking in the Scandinavian-Atlantic sector. It is shown that the oscillation can be viewed as a mode of the non-linear barotropic atmosphere. Three fields are needed in order to simulate the oscillation, i.e., the mean field, an initial anomaly field and a forcing field. All three fields are determined with the aid of the adjoint method by requiring that the oscillation patterns simulated and observed must be as alike as possible. The three fields mentioned have been the unknowns of the problem and the oscillation observed has been the only known variable.

1. Introduction

The spectra of the empirical orthogonal functions (EOF) of the 500 hPa height were studied in Rinne and Sarkanen (1985). The spectral peaks turned out to persist from sample to sample. A description of the phenomena lying behind the peaks was shown to be difficult without deeper study. This was true for the 16-day peak in the spectrum of the second EOF. The peak was finally associated with the classical 16-day wave.

The aim of the present study is to find a description for the 30-day peak in the spectrum of the 8th EOF. The corresponding height pattern is only significant in northern latitudes (the centre of action is at 25° W, 55° N). Because of this fact, and also because of the length of the oscillation, the 30-day peak cannot be directly associated with the well-known 40–50-day oscillation in tropical latitudes (Madden and Julian, 1971, 1972).

One candidate for the present cycle does exist. It is the oscillation described by Sawyer (1970), who found a fluctuation, in the range of 15–60 days, with an "average semi-amplitude" of 80 m at the 500 hPa level over the North Atlantic. Sawyer suggested that the oscillation could be in some way connected with blocking.

In the following, we first present how the oscillation was found in the spectra. The time series studied is then filtered in order to find single oscillations. These, in turn, are used to produce a composite description of spatial oscillation patterns. Finally, a dynamical explanation of the oscillation is sought by trying to simulate the life cycle of those patterns. Our approach can be compared with the case of Rossby waves. The movement of a pattern (Rossby wave) on a background field (constant speed field) is forecast with a non-linear (linear) barotropic model. An additional difficulty is that we do not know that background field. This must therefore be found. Here we will apply the adjoint technique.

2. Spectral description of the cycle

The pattern of the eighth EOF of the 500 hPa height is shown in Fig. 1. The EOFs were computed from a large data set (totally 11876 daily/

* Corresponding author.

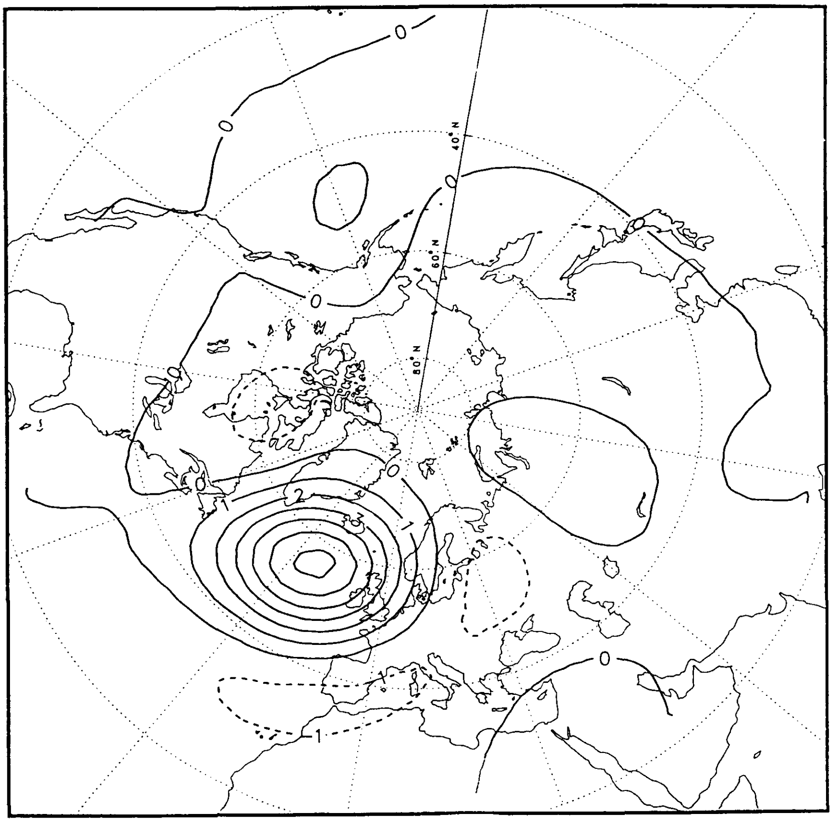

Fig. 1. The 8th EOF of the 500 hPa geopotential height. The field is normalized to unity so that the mean square equals 1.

twice daily analyses from 1946–1970) on a grid of 1404 points north of 20° N (Rinne and Karhila, 1979; Rinne and Järvenoja, 1979; Rinne et al., 1981). The spectrum of the 8th component based on twice-daily analyses for 1962–1970 is given in Fig. 2. The smoothness of the spectrum depends on the length of the prediction error filter employed by the maximum entropy method (MEM, Akaike, 1969). The MEM spectra (Figs. 2a, 2b) and the classical one (Fig. 2c; for details, see Rinne and Sarkanen, 1985) are rather similar. Even the details of Fig. 2a can be traced in Fig. 2c, though a filter of the order of 245 can produce spurious peaks. In these spectra, only the peak at 30 days seems to call for a deeper study. The stability of the peak was further checked by studying its presence in other subsamples: it was similarly found in the spectra computed for 1946–1955, 1956–1962 and 1966–1979.

This 30-day peak is one of the strongest that we have found in the spectra of our EOFs. However, in this paper the spectra will only be used as a guidance to a dynamical study.

3. Identification of individual oscillations

3.1. Band-pass filtering

Time series of the eighth EOF for certain years are shown in Fig. 3. The time series filtered with a 30-day band-pass filter are also shown in Fig. 3. This clearly gives an impression that the 30-day wave explains a lot of the variance. A band-pass filter with a length of 62 days was applied. The

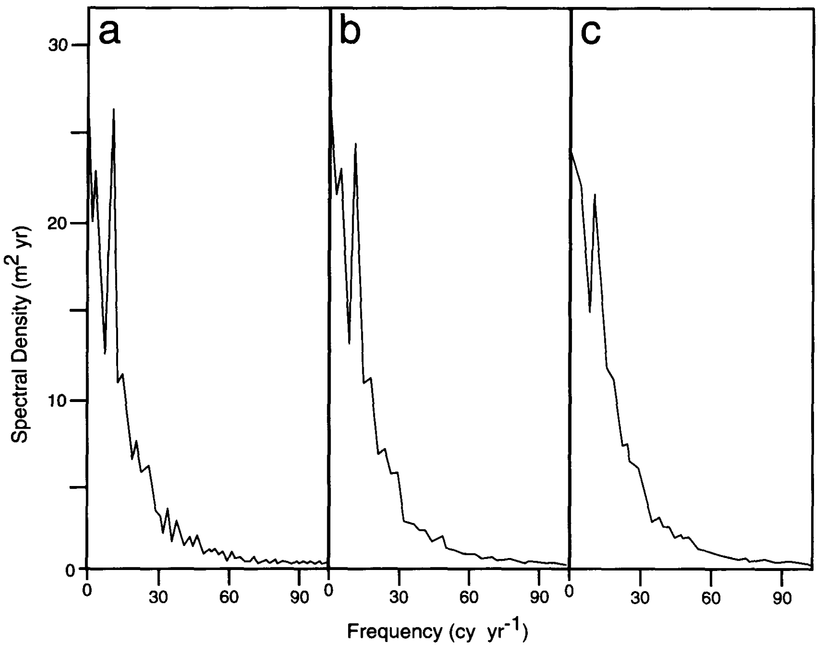

Fig. 2. Three versions of the spectrum associated with the time series of the eighth EOF as observed during 1962–1970. Shown are MEM spectra with filter lengths of (a) 245 and (b) 120 and also (c) the classical spectrum computed with the Parzen window.

smooth response curve of the filter is peaked at 30 days (not shown).

The oscillations (with lengths varying around 30 days) were picked out from the filtered time series. First, the minima and maxima were determined. Weak minima and maxima were neglected. A cycle was arbitrarily defined to begin and end at a minimum. This kind of procedure resulted, for instance, in 1962–1970 in 108 different oscillations having precisely-defined beginning, maximum and ending days.

3.2. *Computation of the composite curve*

A composite curve of the 8th EOF (C_8 in Fig. 4) representing the 30-day oscillation was computed stepwise. First, to find a crude first guess for the oscillation, an average of the 108 oscillations previously mentioned was computed. From each oscillation we cut off the tail exceeding 30 days, after which the average of the remaining 30-day-long pieces was computed. In the building up of composites, we will make use of the non-filtered time series. Only in the construction of this first guess, the beginning dates of the oscillations are taken from the filtered time series.

In the next step, the composite cycle found in this way was allowed to glide over the non-filtered time series of the eighth EOF. Every time the composite fitted well with the time series, an oscillation was noted. Hence in this case the beginning of an oscillation was determined not only by the time of the minimum but by the total fit with the time series. The procedure was repeated by allowing the length of the gliding curve to vary. This was stretched and squeezed so that all periods between 20 and 50 days could be studied. The best fit was used to identify the oscillations. Thus both the beginning day and the length of each oscillation was determined.

From the oscillations identified in the previous search, stretching or squeezing them to a 30-day period, a new composite curve was computed. This was then used as the "gliding identifying tool" of the next step. That composite showed weak kinks (some remnants are still visible in Fig. 4) at the ends of the curve. In the fitting procedure, these

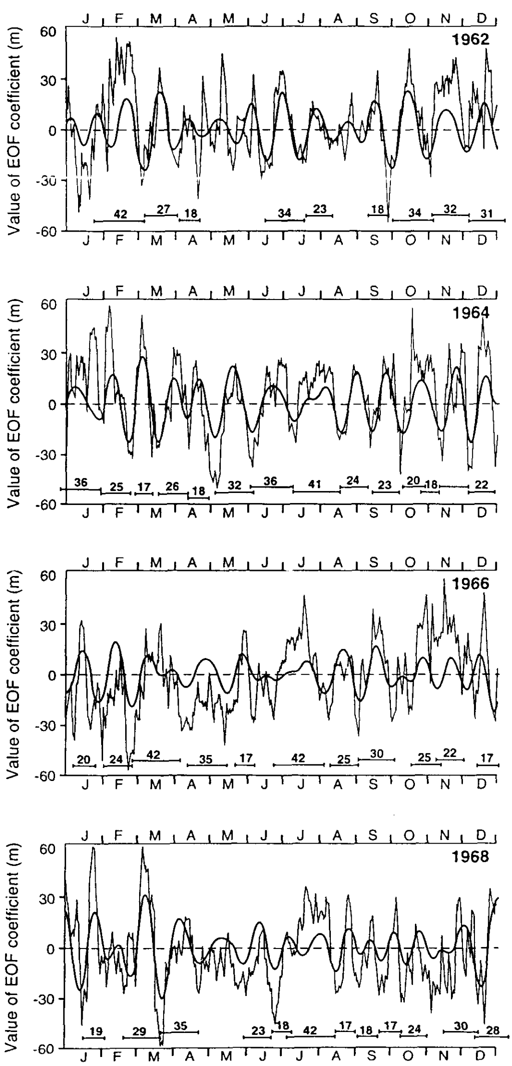

Fig. 3. The variation of the eighth EOF coefficient in 1962, 1964, 1966 and 1968. Thicker lines show the series filtered at 30 days. The cycles identified by the fitting method are indicated by horizontal bars and period lengths in days.

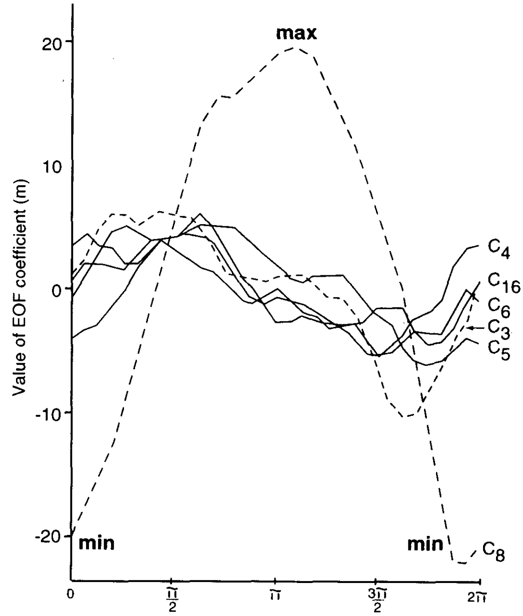

Fig. 4. Composite curves for coefficients of some leading EOFs. Two of the curves (C_3 and C_8) are depicted by broken lines. Values of C_4 have been multiplied by -1.

kinks were cut off. This procedure will not be described here in more detail. However, as a consequence of the cutting, the period range studied became 17, ..., 42 days instead of 20, ..., 50 days.

The procedure was finally repeated by applying the composite curve found in this way. The result did not differ from the previous one indicating that the process had converged. The final result (C_8 in Fig. 4) depicts a nearly sinusoidal cycle with a somewhat flat maximum. Perhaps an additional 15-day cycle is superposed on the 30-day cycle. A minimum is often followed by a rapid increase; hereafter the coefficient varies around the maximum value and finally decreases rapidly.

3.3. *Comments on the filtering and curve fitting*

The cycle lengths often give the interval from the beginning of one cycle to the beginning of the following one. In this sense they seem to be realistic. The sum of the cycle lengths between 27 December 1963 and 31 December 1964 (cf. Fig. 3, 1964) is 363 days. Some cycles slightly overlap, while only a couple of days are not associated with any cycle. In this case the sum of the lengths of the cycles during one year is one year.

The results of the filtering and fitting can be compared in Fig. 3. In the fitting procedure, long cycles will be 42 days long because of the upper limit of the cycle length (42 days). The lower limit, 17 days, causes some short cycles to be neglected. The long cycle at the beginning of 1962 has nevertheless been rather well identified, whereas filtering divides the cycle and nearly smooths it out. In October 1964, the filtering, in turn, seems to perform better. In most cases, the cycles identified through filtering and fitting do not differ much.

4. The 30-day cycle in the other EOFs

Fig. 4 shows composite curves for some leading EOFs. They all tend to show the same cycle. At the minima and maxima, the 30-day cycle is dominated by the eighth EOF. At the zeros of the eighth EOF, other EOFs contribute significantly to the oscillation. The systematic form of the curves and the rather large amplitudes suggest that the cycles in Fig. 4 are significant.

The composite of the eighth EOF is forced to include information from all suitable oscillations. If any kind of noise makes true oscillations longer or shorter, or adds more intensity, the fitting takes such changes into account. Consequently, the composite values describe both true oscillations and red noise. By contrast, in other EOFs the averaging (needed for composite curves) is independent of these EOFs. The picking-up of the

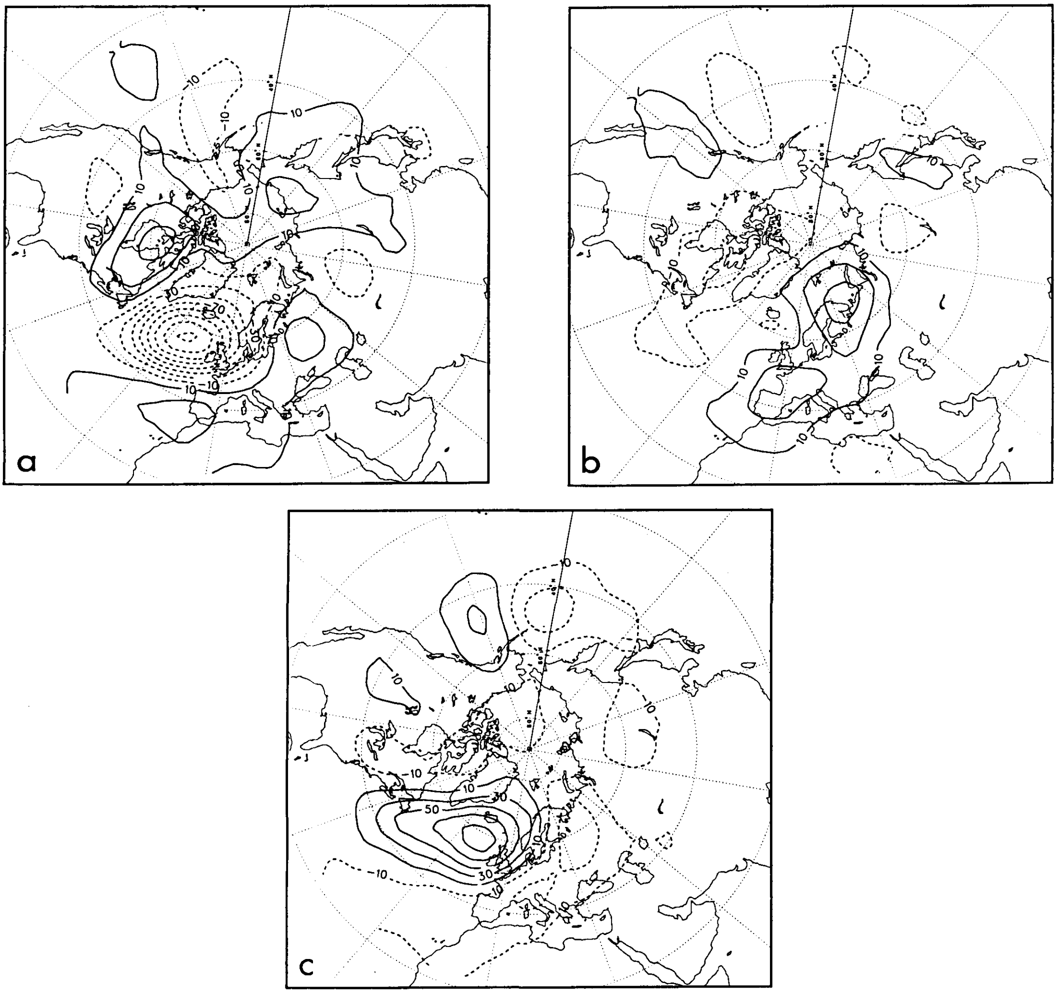

Fig. 5. Composite anomaly maps for 1962–1970 at phases of 0 (a), 8 (b) and 15 (c) days (0, ..., 32 days gives the full cycle).

composite values is fully and only based on the eighth EOF. In such averaging the noise should disappear (assuming that the noise in other EOFs is independent of that in the eighth EOF).

From curves like those in Fig. 4 one can estimate the intensity of the cycle. These values can be compared with the spectral intensities. In order to do that, we estimated the areas of 15- and 30-day peaks in the spectra. The background (red) noise was excluded except in the case of the 8th EOF. The different intensities fit so well that in most of the EOFs the spectral peaks can be explained with the curves in Fig. 4, i.e., with the present cycle. Only in the seventh and ninth EOFs do the composite curves show no cycle, though there are peaks at 15 and 30 days in their spectra (not shown). These peaks thus represent other phenomena.

5. Characterization of the oscillation

Because the beginning day and length of each oscillation are now defined, we can compute corre-

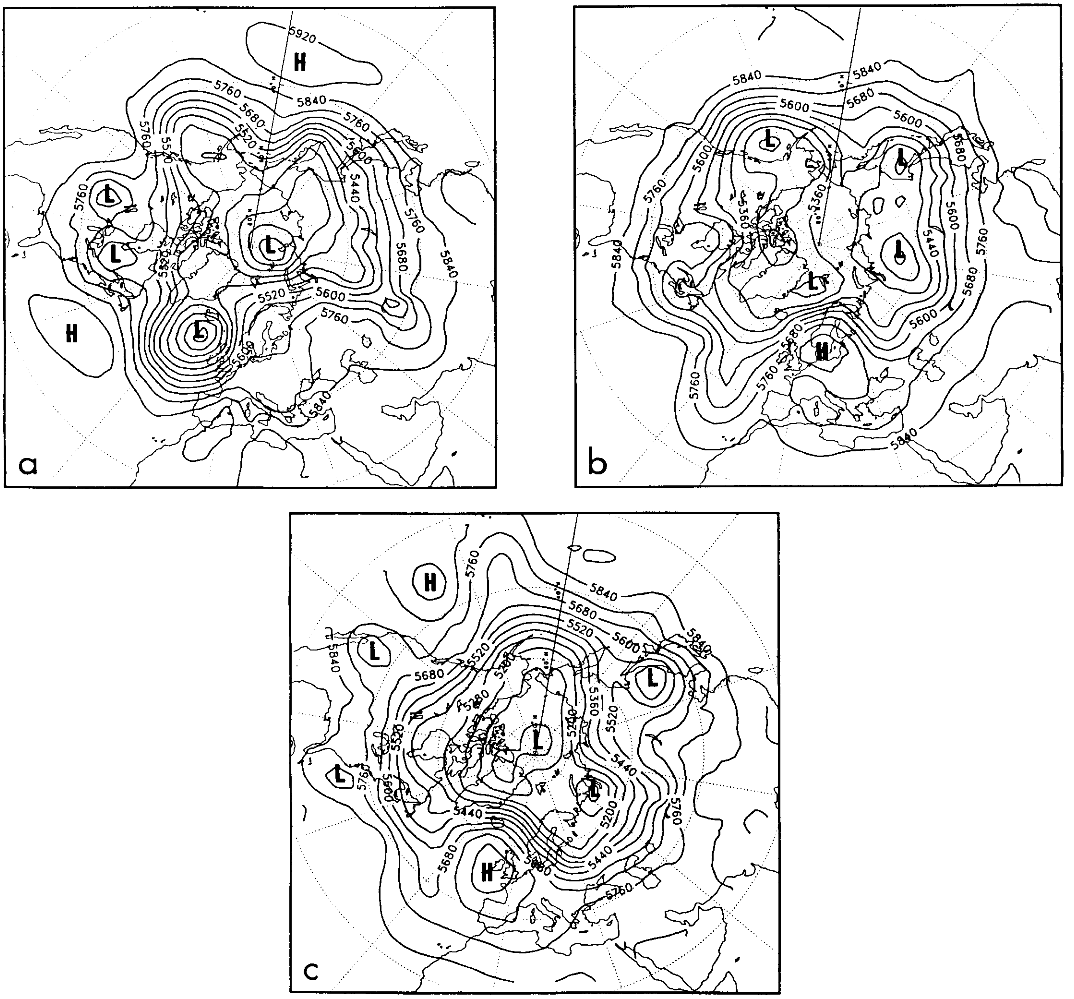

Fig. 6. The 12 UTC height fields of 500 hPa on 30 September (a), 8 October (b) and 19 October, 1962 (c). In terms of a 32-day oscillation as in Fig. 5, the phases in (a), (b) and (c) correspond approximately to phases of 0, 8 and 18 days, respectively.

sponding composite maps by similarly squeezing and stretching the oscillations.

The whole pattern is limited to the Western Europe, Atlantic area (Figs. 5). At the beginning (Fig. 5a), anticyclonic cells are developing over southern and eastern Europe. In the $\pi/2$ phase (Fig. 5b) these have moved north-westward. In the maximum phase (π) the cell is further to the west, over the North Atlantic. From here it continues westward and slowly disappears. Phases of 0 and π present nearly a mirror image. Similarly the development between π and 2π (not shown) is practically a mirror image of that between 0 and π.

The intensity of the oscillation varies. It is at its most intense over the Atlantic (phases of 0, π and 2π). At $\pi/2$ and $3\pi/2$ the main cell is over Scandinavia and is less intense. Thus the oscillation is far from a regular, hemispheric, westward moving wave.

A non-composite case is shown in Figs. 6. The cycle begins on the 30th of September and ends on the 2nd of November 1962. Thus the cycle length is 34 days. The main features of the 30-day oscillation are well shown. There is a strong low over the Atlantic (6a). This is then replaced (6c) by a retrograde blocking approaching from Scandinavia (6b). The cycle shown was one of the 10 strongest during 1962–1970. The weaker cycles cannot be interpreted as clearly as this one.

A histogram showing the distribution of the length of the cycles found by means of the fitting procedure is given in Fig. 7. The columns demonstrating cycle lengths of 17 days (12 cases) and 42 days (8 cases) are not shown because they may include cycles outside the interval 17, ..., 42 days.

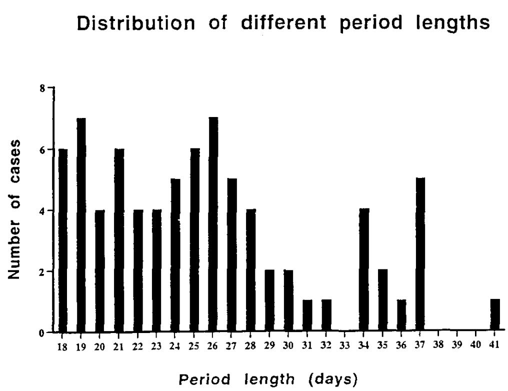

Fig. 7. The histogram of the period lengths observed during 1962–1970.

6. Connection with blocking

The blocking periods during 1962–1969 and their locations in the Atlantic and European sectors were determined subjectively. From these cases we picked out those which appeared over a wide area around the centre of action of the eighth EOF. This area was defined as 0° W–50° W, 45° N–65° N.

About half (48 cases out of 93 in 1962–1969) of the cycles include days with a subjectively-defined blocking. Composite curves of the 8th EOF coefficient for cycles with and without blocking were computed. No essential difference between these curves was observed, although the blocking curve turned out to be somewhat more intense.

Thus the cycle is often associated with blocking. The appearance of blocking does not essentially affect the cycle.

Retrograde blocking highs are typical of Fennoscandia. The descriptions in Namias (1943, 1947) fit our wave well. In particular, the patterns of surface pressure in his Fig. 52 are rather similar to our composite patterns of the 500 hPa height.

7. Comparison to other authors

Cycles or patterns such as the present ones have been found in studies of the zonal index, spherical harmonics or autocorrelation fields. In older studies the data has often been limited.

Namias (1950, his Figs. 2, 3) and Kidson (1985) computed zonal indices indicating an oscillation of some weeks over the North Atlantic. The description given by Kidson fits well with our results: "the cycle has an average period of around 25 days and is most prominent over the Atlantic sector at middle and high latitudes".

Lamb (1972, see pp. 173–179) lists the 30-day wave as one of the best-known higher-frequency waves. Its effects are observed in Europe. Nothing definitive can be said about its connections with the present wave.

In autocorrelation fields a somewhat similar structure has been found by Sawyer (1970; applying a 30-day filter) and Wallace and Gutzler (1981). In the latter paper the term "Eastern Atlantic oscillation" is used. Monthly mean values have been used as data. The 30-day oscillation has therefore been damped. Nevertheless there are similar oscillations. For instance, we have a 49-day oscillation in January 1963, which in Wallace and Gutzler is an intense month in their study. On the other hand, they do not find the nice 22-day oscillation in 1964 (Fig. 3).

Sawyer also determined the movement of the patterns to be northwestwards.

Obviously the results in all three studies (Sawyer, Wallace & Gutzler and the present) overlap. The analysis techniques are very different. Our approach is perhaps more general, as we allow for a wide variation of the period length, we set no a priori geographical limitations and do not require the simultaneous presence of many cells.

In studies based on global modes a clear response at 30 days is found. Those studies often deal with long hemispheric waves and the results are difficult to connect with the patterns of the present local oscillation. Similarities to the present case are: the response is found over the polar latitudes (Krishnamurti and Gadgil, 1985); it is often present and moves westward (Weber and Madden, 1993); there is an important role for westward-propagating long waves in the blocking process (Lejenäs and Madden, 1992).

Patterns oscillating at 30 days are also found elsewhere. These may be similar in character, partly overlapping or in some way connected to the present oscillation. When studying the 40- to 50-day tropical oscillation (Madden and Julian, 1971, 1972), Weickmann et al. (1985, their Figs. 6, 9) show an additional North Atlantic fluctuation moving westward. Further, a connection between the tropical and northern oscillations has been suggested by Gutzler and Madden (1993). On the other hand, Strong et al. (1993) demonstrate that (standing) modes at 35–50 days over Northern Hemisphere midlatitudes could be induced by topographic instabilities.

Branstator (1987) described a 25-day oscillation over the western part of the Northern Hemisphere. The corresponding spectrum much resembles that found in our case. Some patterns resemble ours. The 45-day mode analyzed by Ghil and Mo (1991) partly shows patterns comparable to our oscillation.

A westward-propagating disturbance over the Pacific, with a period of the order of three weeks, has been simulated and observed by Kushnir and Esbensen (1986). It resembles ours: "The Pacific disturbance propagates slowly westward and its period is of the order of 3 weeks".

8. Modelling of the oscillation

8.1. Modelling without forcing

The literature review shows that the present oscillation has obviously been found earlier, but not very often. It has been observed to be local to the European-Atlantic sector with a period of about a month, perhaps connected to blocking. Otherwise it has been difficult to characterize, the patterns and movements differing in different studies. No explanation for the oscillation has been given.

In the following we try to view the oscillation as a mode of the barotropic atmosphere. We apply the vorticity equation for 500 hPa. The computation area is shown in Fig. 1 and the grid interval is 381 km at 60° N. We make forecasts for the range of $0-\pi$, i.e., from the minimum to maximum (cf. curve C_8 in Fig. 4). From the forecasts, the average and, with the aid of this, the daily anomalies are computed. If the observed and simulated anomalies coincide, then a model description of the oscillation has been found.

Thus the task is to find a suitable set of forecasts (if such a set exists). The forecasts are completely determined by the initial condition, which should therefore be found. This is done by applying the adjoint technique in a grid-point model (Rinne and Järvinen, 1993; Järvinen, 1993). We take an initial guess and compute the forecasts and anomalies from it. The root mean square difference between the forecasted and observed (composite) anomalies is then computed. This is our penalty function that must be minimized with respect to the initial field. This initial field is implicitly present in the penalty function because the forecasted anomalies depend on it via the model. Note that the anomalies are computed from forecast-minus-mean, where the mean field, in turn, depends on the forecasts. The adjoint model advises how the initial guess must be changed in order to make the value of the penalty function smaller.

The adjoint approach requires considerable computing time. Therefore a shorter oscillation period is preferred. We choose a period of 16 days. From Figs. 3, 7 one can see that such shorter periods are present in our oscillation. Obviously it is enough to make simulations from the minimum to the maximum phase. Accordingly, we try to simulate the development of the composite anomaly patterns so that they change from the minimum to the maximum phase during 8 days.

As a result of the adjoint computations, we found an initial field to be used in the making of the forecasts. The mean field (Fig. 8b) computed from the forecasts (incl. the initial field) is rather close to that observed (Fig. 8a). Differences are seen over the Pacific and in details, such as a ridge west of Iceland which is not present in the simulated field. Note that the input for our computations include only the anomalies, apart from which there has been no climatogical input. Thus the mean field in Fig. 8b is found on the basis of the anomalies and the model.

The forecast anomalies (not shown), computed as deviations from the simulated mean field, are close to the observed anomalies, as required by the penalty function (numerical r.m.s. values given in Section 9).

Thus there exists, in the equivalent barotropic atmosphere, a mode, associated with a mean field, such that both the mode and the mean field are close to those observed in the real atmosphere. The present oscillation can thus, approximately, be

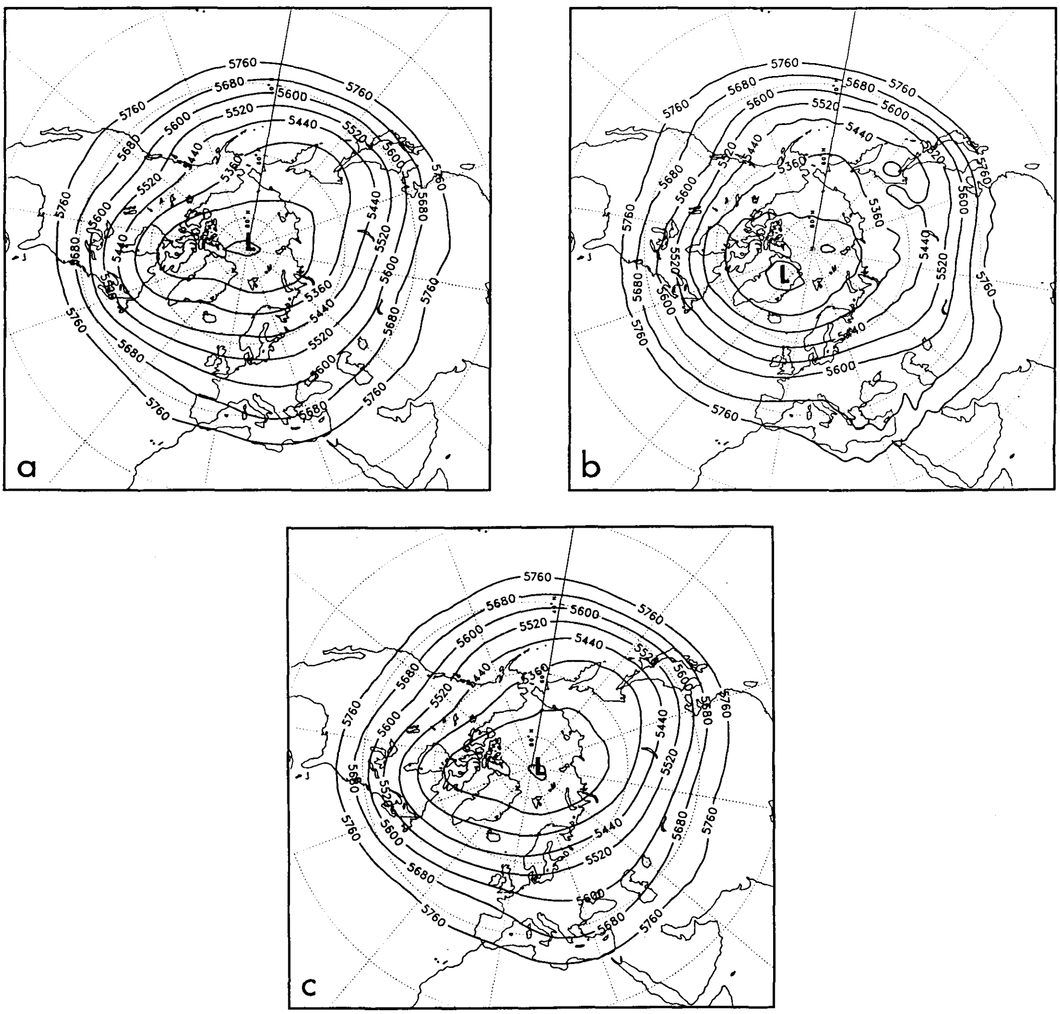

Fig. 8. The mean fields observed (a), simulated (b) without forcing and (c) with forcing.

seen as a mode of a non-linear barotropic atmosphere.

The experiment shows that we cannot, in the simulation, apply observed fields as such. The observed and simulated fields differ from each other, both in the case of initial anomalies and mean flow. The differences are rather small but, nevertheless, essential for a successful simulation.

8.2. Modelling with forcing

The differences between the mean fields observed and simulated in the previous experiment perhaps reflect some kind of forcing. We therefore added one more equation. The height tendency will be computed from the model as previously. However, forcing effects will then be simulated to give the final height tendency as follows:

$$\partial z/\partial t(i,t)_{\text{final}} = \partial z/\partial t(i,t)_{\text{model}} + \partial z/\partial t(i)_{\text{forcing}}.$$

Here i and t refer to the gridpoint and time. Note that the forcing term is independent of time.

The task is now to find two unknown fields. These are the initial field of the computations and a forcing ($\partial z/\partial t(i)_{\text{forcing}}$) field, which affects similarly at every time step.

The results of this (in principle) simple experiment were surprisingly satisfactory. As previously, the anomalies observed and simulated coincide well. However, in this experiment this is true for the mean conditions as well, even small details being reconstructed (Fig. 8c).

The gradients in the forcing field (Fig. 9a) reflect the sea-continent distribution of the Northern Hemisphere. There is one exception, that of the Atlantic sector. Note that the southernmost patterns in Fig. 9 are not reliable because they represent nothing more than boundary errors.

Our model applies the so-called Cressman term (0.75×10^{-12} m^{-2}), which is usually seen as a term due to the divergence associated with the long waves. We made experiments in which the value of this parameter was varied. The main change in the results was in the intensity of the mean flow. The Cressman term seems therefore to be of minor importance.

The gradients in the forcing field tend to follow continental coastlines. Obviously the main factor in the field is the contrasts between the oceans and the continents. One can also see a reflection of the polar cap. The Rocky Mountains and Himalayas can perhaps be traced in the map. The forcing field may be a combination of many factors which seem to be connected to the forcing due to synoptic scale transients (Sheng, 1994).

The North Atlantic sector represents an exception to the general geographical description of the forcing field. Because of this deviation, one may think that we have here the specific conditions required to maintain the present 30-day oscillation. Therefore we next separate the forcings needed to maintain the mean field and the oscillation. There are two ways of doing this.

First, we can make a forecast applying only the mean field as the initial field and then determine the forcing so that no anomalies are generated, i.e., the tendencies vanish. The result will be exact.

Secondly, we can repeat the full adjoint process by requiring that all forecasts equal the mean field. This will not be completely fullfilled and the resulting forcing field will only be an approximation. However, the computations are similar to the main case. For instance, an additional penalty term with its smoothing effect (described later in Section 9) is included. The different forcing fields are therefore easier to compare.

To determine the forcing field (Fig. 9b) required to maintain the mean field, we applied the second method. By subtracting the field in Fig. 9b from the one in Fig. 9a, we found the anomalous forcing field (Fig. 9c) needed to maintain the 30-day wave.

Once again, the result is surprising. The anomalous forcing field much resembles the eighth EOF in Fig. 1, the only essential differences being found over the Pacific. In the Atlantic sector, the centre of action is more westward in the response field (Fig. 1) than in the forcing field. This sounds reasonable for a westward-moving mode.

Although Figs. 1 and 9c are similar, there is one important principal difference. The forcing field (9c) does not change with time whereas the response varies. In fact, the variation in the eighth EOF was used in the identification of the 30-day wave.

Because the mean field in Fig. 8c is so similar to that observed (8a), the result can be considered reasonable. As the waves in the mean field are so dominant, the forcing field required to maintain the mean field must be uniquely given. The residual part, i.e., the forcing field required to simulate the 30-day wave, may vary more. One can even simulate without the forcing field, although

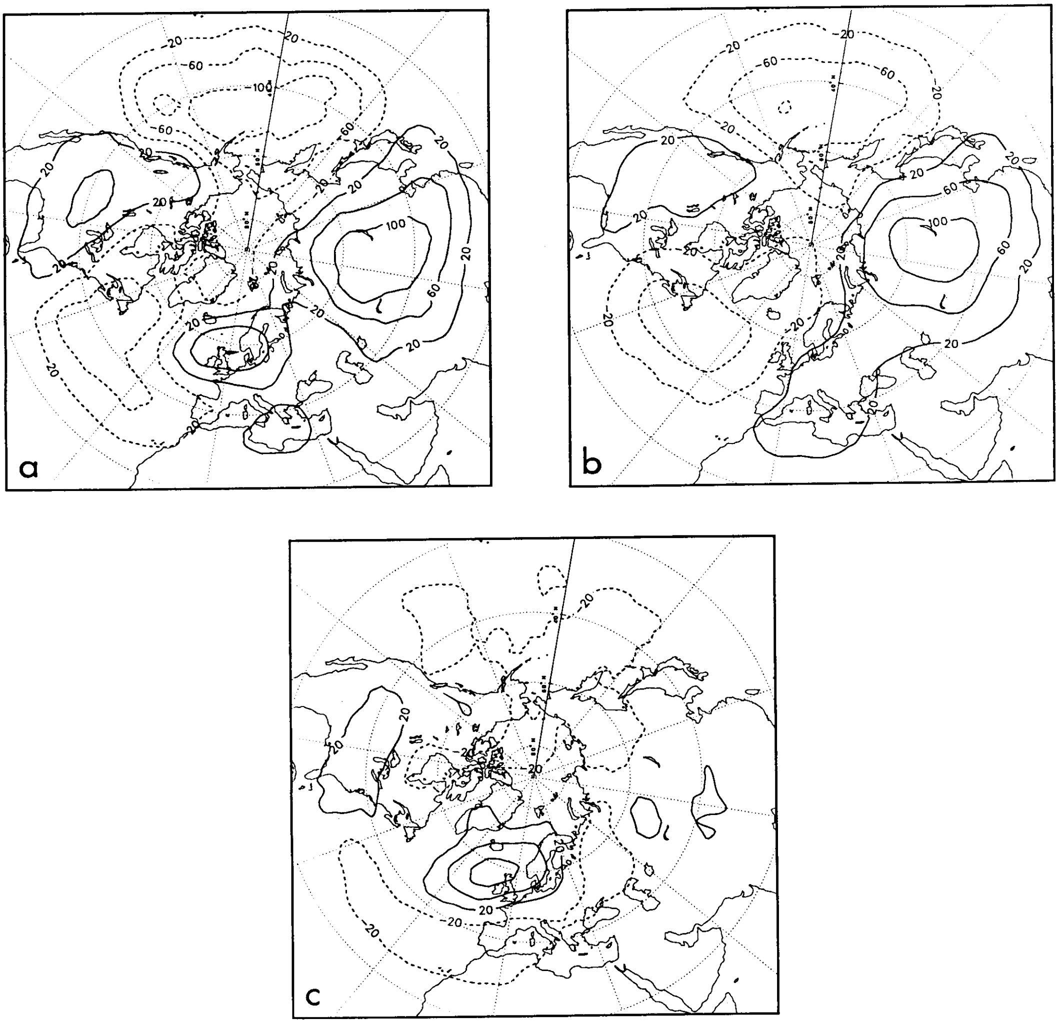

Fig. 9. Forcing fields required to simulate the oscillation (= anomalies + the mean field) (a), to maintain the mean field (b) and to produce the anomalies on the mean field (c). The last field is computed as the difference of the previous two. Units: cm/h.

modifications in the mean field are then required. On the other hand, computations with different initial guesses, with different Cressman terms and with a different penalty term (with or without smoothing) result in similar forcing fields. Therefore, only one solution seems to exist. The more we move from this solution, the worse the simulation becomes.

The residual forcing contributes mainly over the Atlantic, indicating that the solution is reasonable. In nature this forcing may vary a lot because the 30-day wave itself varies considerably.

Finally we recall the input and output of our system. The only information fed into the system has been the assumption of constant absolute vorticity, the rotation of our planet, the Cressman term, and the anomalies of a local oscillation observed at one level in the atmosphere. No information about the mean flow, mountains, continents nor oceans is given. From this input we have derived the mean flow of the atmosphere and a forcing field. This in turn reflects geographical patterns at the surface of the planet.

9. Comments on the application of the adjoint approach

There are three fields acting in our model atmosphere, those representing the mean flow, the anomaly, and forcing. In order to obtain a successful simulation in a non-linear atmosphere, these must be suitably balanced. If no forcing is applied, then the mean field needed (Fig. 8b) will be a modified version of the observed one (Fig. 8a). If forcing is applied, then the mean field (Fig. 8c) will be similar to the observed one. In both cases (forcing and no forcing), the anomaly field used to start the simulation must be suitably adjusted. If we make a conventional forecast, applying the barotropic model without forcing and starting from the observed field, then the balance needed between the three components disappears. The movement of the mean field becomes dominant, and the forecasts do not simulate the anomalies observed. Without mutually-balanced fields, i.e., without adjoint computations, no successful simulation can be performed.

The adjoint modelling was based on the work done in Rinne and Järvinen (1993) and especially in Järvinen (1993). The latter paper deals with an automatic way to develop a program code for the adjoint computations. This method is applied here. It includes a careful verification of all parts of the program.

In the absence of a forcing field, there were no problems in the computations. Starting with a suitable initial field, the initial r.m.s. difference decreased from 848 m^2 to 110 m^2. These values are given as an average of 9 fields (8 day forecasts + the initial field) and of 1404 grid points.

To avoid boundary problems, we applied smoothing at the boundaries. In the case of applying a forcing field, difficulties arose. While varying the initial guess or the convergence parameters, different solutions appeared. Sometimes the convergence was very rapid. The solutions were not satisfactory. On a reasonable basic structure, different kinds of "grid point storms" were found to be superposed.

The problem was interpreted as non-identifiable. All the different results represented nothing but solutions of different local minima. From these obviously numerous solutions we wished to choose the smoothest one. We added the square Laplacian of the forcing field to the penalty term. The additional term was first multiplied by a suitable small constant. Now there were no more problems. The initial r.m.s. difference decreased from 848 m^2 to 118 m^2. In the latter value, only 4 m^2 was contributed by the additional new term. Hence this term obviously had no essential effect on the solution, but only helped in selecting a smooth solution. The smoothing effect is visible in all the fields. The experimental results are not shown in more detail. However, the presence and absence of the noise in Figs. 8b and 8c illustrate cases without and with the additional penalty term, respectively.

The simulations were performed for an oscillation of 16 days. Forecast runs longer than 8 days (i.e., oscillation periods longer than 16 days) were not successful. Our simulation studies therefore tell nothing about the factors that cause the oscillation period to vary. According to the classical linear theory, the main factor should be the intensity of the background flow.

10. Conclusions

A spectral peak at a period of 30 days found in the time series of a certain EOF has been studied. Single cycles of the oscillation have been identified in order to produce composite curves describing the oscillation.

The identification of the cycles was first made by assuming a period length of 30 days and determining the cycle beginnings from the filtered time series. The resulting composite curve shows a sinusoidal cycle. Secondly, the composite curve so found was allowed to glide over the non-filtered time-series. Where a good fit was found, a cycle was marked. In the 3rd run, the period length of the gliding curve was allowed to vary. This third method was especially aimed at determining the period length of the actual cycle.

The oscillation turns out to consist of westward-moving cells over the Atlantic. The oscillation is often associated with a blocking over the British Isles. In such cases, the concept of a retrograde Scandinavian-Atlantic blocking is appropriate.

As a successful application of the adjoint method, it has been shown that the oscillation can be viewed as a mode of the non-linear barotropic atmosphere. As input we have used the assumption of constant absolute vorticity, the rotation of our planet, the Cressman term, and the anomalies of a 30-day oscillation observed at 500 hPa. There has been no inclusion of information about the mean flow, mountains, continents or oceans. With the aid of the adjoint method, we have derived the mean flow and a forcing field needed in the generation of the oscillation. The mean flow so found is nearly a "carbon copy" of that observed. The forcing in turn reflects geographical patterns at the surface of the planet.

Finally, the forcing field is divided into two parts, that needed to maintain the mean field and that to generate the oscillation on the mean field. The latter part of the forcing turns out to be local to the Atlantic.

A computational difficulty was encountered in the adjoint computations. The problem appeared to be non-identifiable. This was solved by adding a smoothing term to the penalty function, which helped to select a reasonable solution.

11. Acknowledgements

The adjoint computations were made using a program that Heikki Järvinen especially modified for this case. We are grateful for this professional work which made it possible to carry out this study. Once again Robin King helped us by reading the manuscript. Finally we will thank the referees for their help, especially Professor Jon Ahlquist.

REFERENCES

Akaike, H. 1969. Power spectrum estimation through autoregressive model fitting. *Ann. Inst. Stat. Math.* **21**, 407–419.

Branstator, G. 1987. A striking example of the atmospheric leading traveling pattern. *J. Atmos. Sci.* **44**, 2310–2323.

Ghil, M. and Mo, K. 1991. Interseasonal oscillation in the global atmosphere. Part I: Northern hemisphere and tropics. *J. Atmos. Sci.* **49**, 752–779.

Gutzler, D. and Madden, R. 1993. Seasonal variations of the 40–50-day oscillation in atmospheric angular momentum. *J. Atmos. Sci.* **50**, 850–860.

Järvinen, H. 1993. *A direct conversion of model algorithms to their adjoints exemplified with a barotropic atmospheric model.* Report no. 42, Department of Meteorology, University of Helsinki, Finland, 41 pp.

Kidson, J. 1985. Index cycles in the northern hemisphere during the global weather experiment. *Mon. Wea. Rev.* **113**, 607–623.

Krishnamurti, T. and Gadgil, S. 1985. On the structure of the 30 to 50 day mode over the globe during FGGE. *Tellus* **37A**, 336–360.

Kushnir, Y. and Esbensen, S. K. 1986. *Diagnosis of low-frequency, extratropical disturbances in a two-level general circulation model.* Long-Range Forecasting Research Reports Series No. 6 (WMO/TD No. 87), 521–529.

Lamb, H. 1972. *Climate: present, past and future*, vol. 1. Methuen & Go Ltd., London, 613 pp.

Lejenäs, H. and Madden, R. 1992. Traveling planetary–scale waves and blocking. *Mon. Wea. Rev.* **120**, 2821–2830.

Madden, R. and Julian, P. 1971. Detection of a 40–50 day oscillation in the zonal wind in the tropical Pacific. *J. Atmos. Sci.* **28**, 702–708.

Madden, R. and Julian, P. 1972. Description of global scale circulation cells in the tropics with a 40–50 day period. *J. Atmos. Sci.* **29**, 1109–1123.

Namias, J. 1943. *Methods of extended forecasting.* US Weather Bureau, Washington DC, 64 pp.

Namias, J. 1947. *Extended forecasting by mean circulation methods.* US Weather Bureau, Washington DC, 55 pp.

Namias, J. 1950. The index cycle and its role in the general circulation. *J. Meteor.* **7**, 130–139.

Rinne, J. and Järvenoja, S. 1979. Truncation of the EOF series representing 500 mb heights. *Quart. J. Roy. Meteor. Soc.* **105**, 885–897.

Rinne, J. and Järvinen, H. 1993. Estimation of the Cressman term for a barotropic model through optimization with use of the adjoint model. *Mon. Wea. Rev.* **121**, 825–833.

Rinne, J. and Karhila, V. 1979. Empirical orthogonal functions of 500 mb height in the Northern Hemisphere determined from a large data sample. *Quart. J. Roy. Meteor. Soc.* **105**, 873–884.

Rinne, J., Karhila, V. and Järvenoja, S. 1981. *The EOFs of the 500 mb height in the extratropics of the Northern Hemisphere*. Report No. 17, Department of Meteorology, University of Helsinki, 00100 Helsinki 10, Finland, 16 pp. + Appendix, suppl., 88 pp.

Rinne, J. and Sarkanen, A. 1985. 500 mb geopotential height spectral peaks in the 1- to 5-week range. *Tellus* **37A**, 323–335.

Sawyer, J. S. 1970. Observational characteristics of atmospheric fluctuations with a time scale of a month. *Quart. J. Roy. Meteor. Soc.* **96**, 610–625.

Sheng, J. 1994. *Assessment of the Interactions between slow transients and synoptic-scale eddies in a T32 general circulation model.* #2.43 in: Research activities in atmospheric and oceanic modelling (ed. G. J. Boer). Report no. 19 by CAS/JSC Working Group on Numerical Experimentation. WMO/TD, no. 592.

Strong, C., Fei-Fei Jin and Ghil, M. 1993. Intraseasonal variability in a barotropic model with seasonal forcing. *J. Atmos. Sci.* **50**, 2965–2986.

Wallace, J. M. and Gutzler, D. S. 1981. Teleconnections in the geopotential height field during the northern hemisphere winter. *Mon. Wea. Rev.* **109**, 784–812.

Weber, R. and Madden, R. 1993. Evidence of traveling external Rossby waves in the ECMWF analyses. *J. Atmos. Sci.* **50**, 2994–3007.

Weickmann, K., Lussky, G. and Kutzbach, J. 1985. Interseasonal (30–60 day) fluctuations of outgoing longwave radiation and 250 mb streamfunction during northern winter. *Mon. Wea. Rev.* **113**, 941–961.